

---

# QUANTIZED-TINYLLAVA: A NEW MULTIMODAL FOUNDATION MODEL ENABLES EFFICIENT SPLIT LEARNING

---

**Jiajun Guo**  
Department of Statistics  
University of Michigan  
Ann Arbor, MI 48109  
gjiajun@umich.edu

**Xin Luo**  
Gilbert S. Omenn Department of Computational Medicine & Bioinformatics  
University of Michigan  
Ann Arbor, MI 48109  
luosan@umich.edu

**Jie Liu**  
Gilbert S. Omenn Department of Computational Medicine & Bioinformatics  
University of Michigan  
Ann Arbor, MI 48109  
drjieliu@umich.edu

December 1, 2025

## ABSTRACT

Split learning is well known as a method for resolving data privacy concerns by training a model on distributed devices, thereby avoiding data sharing that raises privacy issues. However, high network communication costs are always an impediment to split learning, especially for large foundation models that require transmitting large amounts of high-dimensional data. To resolve this issue, we present a new multimodal model structure that incorporates a learning-based data compression method, which compresses model embeddings into low-bit integers while preserving the model’s performance, greatly reducing the transmission costs between partitions. We then determine the optimal number of discrete representation levels based on a solid theoretical foundation from entropy coding. The code is available at <https://github.com/Gjj-114514/Quantized-tinyllava>.

## 1 Introduction

Training large foundation models requires aggregating massive, heterogeneous datasets to achieve robust generalization across domains. However, accessing such data often raises serious privacy and regulatory concerns, especially when sensitive or proprietary information is involved [1]. This creates a fundamental tension between the need for diverse training data and the obligation to protect confidentiality. As a result, there is a growing push toward collaborative model development under strict privacy constraints. For instance, hospitals seek to jointly train pathology models without sharing patient records; financial institutions aim to build credit risk models while preserving client anonymity; and computational biology centers must train genomic models where whole-genome sequencing (WGS) data remain confined to secure local servers.

In response, privacy-preserving machine learning paradigms have garnered increasing attention. Among them, split learning has emerged as a promising framework that enables collaborative model training without exposing raw data [2]. In this scheme, the model is partitioned between clients and a central server. While this method effectively decouples data ownership from model inference and reduces privacy risks, it introduces substantial communication overhead due to the transmission of high-dimensional intermediate features and gradients. Numerous split learning frameworks have been proposed, addressing the communication overhead problems and data leakage concerns. However, none of them is efficient enough for large foundation models due to complex features and tasks.

In foundation models, quantization has been proposed as an effective technique for compressing data. Many studies have demonstrated that foundation models can maintain performance under 8-bit quantization [3] for intermediate

features. However, higher compression rate (e.g., 4-bit, 2-bit) still inevitably causes information loss thereby degrading model’s performance [4]. To achieve further compression, discrete representation learning with neural networks offers a promising approach. Among deep learning models, one of the most representative methods is VQ-VAE. It utilizes an encoder to produce continuous vectors and then maps them to a set of discrete codes via a learnable codebook, effectively compressing the data into compact, discrete representations. [5]. However, VQ-VAE suffers from significant limitations, including the codebook collapse problem and high computational complexity. To address these issues, the recently proposed Finite Scalar Quantization (FSQ) method serves as a simpler yet effective alternative, leveraging a straightforward rounding operation and the straight-through estimator. [6].

Despite extensive research, to the best of our knowledge, no well-established multi-modal foundation model architecture has been proposed that incorporates a split learning strategy through vector quantization. Moreover, to implement vector quantization technique into a large foundation model, there are still problems to solve. Compared with ordinary deep learning models, large foundation models require encoding complex contextual structure and learning from complex information. This could require a higher degree of information preservation. Moreover, determining the optimal quantization bandwidth has been a long challenge that is highly dependent on empirical heuristics and extensive experiments.

To address this issue, we proposed a new multi-modal foundation model that incorporates a novel vector quantization method. This method retains the simplicity and computational efficiency of FSQ but achieves a significantly higher compression rate while maintaining model performance, thereby enabling more efficient split learning. Built upon the TinyLLaVA framework [7], we presented a general framework for constructing, evaluating, and analyzing quantized multi-modal foundation models. Then, we established a theoretical foundation for determining the optimal number of discrete representation levels based on entropy coding theory, which was subsequently validated through our experiments.

## 2 Related Work

### 2.1 Split learning

The concept of split learning was first presented by Gupta in 2018 [2]. Its core idea is to distribute deep neural network models across multiple entities and train over several data sources to address the issue of limited computational resources and data privacy. The main concern for this method lies in its communication efficiency and the risk of data leakage. Regarding its privacy problem, Ngoc et al. introduced differentially private in split learning and studied the trade-off between privacy protection and model performance [8]. Jiang et al. resolved the label leakage problem through dimension transformation [9]. Meanwhile, to address the communication bottleneck, Zheng et al. presented random top-k sparsification improving model’s performance under certain compress rate [10]. Oh et al. introduced SplitFC that involves multiple methods including adaptive dropout and quantization to reduce feature transition [11].

Despite extensive research on this topic, existing approaches have not been effectively applied to large foundation models, which involve more complex tasks and feature representations. Our work aims to bridge this gap by introducing a novel foundation model architecture tailored for such large-scale, multi-modal settings.

### 2.2 Multi-modal foundation model

With an emerging trend of general AI and big-data, large foundation model has become a focus with numerous language models such as GPT [12], Phi [13], Openelm [14], Qwen [15] and vision model such as Siglip [16], Clip [17]. LLaVA [18] provided an effective methodology for constructing a multi-modal foundation model. It utilized a linear connector that maps features from the vision modality into the language modality. Based on this, Zhou et al. [7] presented TinyLLaVA, providing a unified and modular framework for convenient design and analysis of small-scale multi-modal foundation models.

### 2.3 Quantization

To reduce the space consumption issue in large foundation models, numerous quantization methods had been proposed. In `llm.int8()` [3], the weight and activation values of the model was quantized to 8-bit integer without significant drop in performance. Qlora [19] proposed a new quantization method leveraging 4-bit NormalFloat and double-quantization successfully compressed model’s weight to 4-bit. However, none of these works had successfully compressed intermediate features lower than 4-bit.

## 2.4 Discrete Representation Learning

Unlike quantization, discrete representation learning compress data by learning meaningful discrete latent codes from data. One of the most representative methods is the Vector Quantized Variational Autoencoder (VQ-VAE), first introduced by van den Oord et al. [5]. Its core idea is to mapping continuous features from the encoder to a discrete latent space by learning a codebook  $\mathcal{C}$ , which provides an effective discrete learning method for high-dimensional data, thereby improving the quality and efficiency for generation tasks. In 2019, Razavi et al. [20] improved VQ-VAE by introducing Hierarchical Latent Structure to capture features at different scales. Moreover, Esser et al. [21] presented a VQ-VAE structure that is integrated with a Vision Transformer model, demonstrating VQ-VAE’s compatibility with transformer-based models.

However, VQ-VAE is still limited by its complex computation, unstable training and problems of codebook-collapse. Compared to VQ-VAE, finite scalar quantization (FSQ) provides a simple yet efficient discrete learning method [6]. This approach obtains discrete codes from features by scaling vector values to preset levels and then rounding them to integers, which proves to be as effective as VQ-VAE while overcoming its limitations. Since the  $\text{round}()$  operation is non-differentiable, the straight-through estimator (STE) is commonly employed to approximate the gradient of the rounding operation. The resulting gradient estimate is formulated as follows:

$$y = \text{round}(x) \text{ (forward)}$$

$$\frac{\partial L}{\partial x} = \frac{\partial L}{\partial y} \text{ (backward)}$$

Experiments have demonstrated that Finite Scalar Quantization (FSQ) performs as effectively as VQ-VAE on various vision tasks using MASKGIT and UViM, including image generation, depth estimation, colorization, and panoptic segmentation. However, the overly simplified procedure of FSQ may give rise to certain challenges that are largely hidden by the continuous nature of image data, which places weaker demands on information preservation. Moreover, there has not yet been a well-established criterion for determining the quantization levels in FSQ, resulting in a strong reliance on repeated experimentation and empirical heuristics. A more detailed analysis of these issues will be provided in subsequent sections.

## 3 Methods

### 3.1 Data Compression

In our work, we presented a learning-based data compression method on the basis of FSQ. The computation algorithm of FSQ shown in Algorithm 1. The discrete codes are obtained by implementing rounding operations to encoded features.

---

#### Algorithm 1 FSQ procedure

---

**Initialize:** Encoder  $\mathcal{E}_\phi$  with parameter  $\phi$   
**Input:** data  $X$  and number of discrete representation levels  $K$ ;  
**Output:** Quantized feature  $C$ ;

- 1:  $e \leftarrow \text{Tanh}(\mathcal{E}_\phi(X))$ ;
- 2: **if**  $K$  is odd **then**
- 3:    $z \leftarrow \text{round}(\frac{K-1}{2}e)$
- 4: **else**
- 5:    $z \leftarrow \text{round}(\frac{K-1}{2}X - 0.5) + 0.5$   
     (ensure  $z$  is symmetric around 0 )
- 6: **end if**
- 7:  $I \leftarrow z + \frac{K-1}{2}$
- 8:  $C \leftarrow (I - \frac{K-1}{2}) / \frac{K-1}{2}$

---

This algorithm is executed on both the clients and the server. On the client side, positive integer indices  $I$  are generated and transmitted to the server for network communication. Upon receiving  $I$ , the server reconstructs the corresponding continuous representations  $C$  by scaling  $I$  to the range  $(-1, 1)$ , which are then used for the remainder of the forward

propagation.

With respect to FSQ, we identified several limitations and developed corresponding improvements to address them.

### Linear scaling

FSQ employs  $Tanh()$  function to scale vector values into  $[-1, 1]$  for quantization. However, this method is potentially problematic by shaping the distribution of activations into a highly bimodal form. This distribution, with its sharp peaks at the saturation boundaries (-1 and 1) and negligible density in intermediate regions, leads to two critical issues. First, it results in severe under-utilization of the codebook, as the vast majority of quantization levels remain unused, thereby degrading the model’s effective representational capacity. Second, it exacerbates the vanishing gradient problem during training, as most activations reside in the gradient-saturated regions of the tanh function, impeding effective learning. We found that a linear operation turns out to be better. The calculation is as follows:

$$scale(x) = 2 \frac{X - \max(X)}{\max(X) - \min(X)} - 1 \in (-1, 1)$$

To mitigate the influence of outliers, before scaling, we first limit the vector values into bound:

$$[\mu_X - 3 * \sigma_X, \mu_X + 3 * \sigma_X]$$

where  $\mu$  and  $\sigma$  are the mean and standard derivation of input features  $X$ .

### Distortion regularization

In FSQ, the input features are directly rounded to integer values, which can introduce distortion relative to the original features, particularly when the number of discrete levels is small. Since the straight-through estimator is used to approximate the gradient, it is crucial to minimize the discrepancy between the pre- and post-rounding values to ensure accurate gradient estimation. To this end, we introduce a commitment loss term that penalizes deviations from the original features, formulated as:

$$L_{comm} = (1 - \cos(\frac{K-1}{2}e, sg(z)))$$

where:

$$\cos(a, b) = \frac{a^T b}{\sqrt{a^T a b^T b}}$$

Here, we employ a cosine similarity loss to measure the distortion arising from the high dimensionality of the embedding.  $sg()$  denotes the stop-gradient operation. This term ensures that the discrepancy between the rounded and original values remains small, thereby enabling an accurate estimation of the gradient.

Above all, our new quantization procedure is formulated as in Algorithm.2:

---

#### Algorithm 2 Our method

---

**Initialize:** Encoder  $\mathcal{E}_\phi$  with parameter  $\phi$ , commitment cost  $\alpha$

**Input:** data  $X$  and level number  $K$ ;

**Output:** Quantized feature  $C$ , commit loss  $L_{comm}$ ;

- 1:  $e \leftarrow \text{scale}(\mathcal{E}_\phi(X))$ ;
  - 2: **if**  $K$  is odd **then**
  - 3:    $z \leftarrow \text{round}(\frac{K-1}{2}e)$
  - 4: **else**
  - 5:    $z \leftarrow \text{round}(\frac{K-1}{2}X - 0.5) + 0.5$
  - 6: **end if**
  - 7:  $I \leftarrow z + \frac{K-1}{2}$  (Transfer from clients to server)
  - 8:  $C \leftarrow (I - \frac{K-1}{2}) / \frac{K-1}{2}$  (Received at server)
  - 9:  $L_{comm} \leftarrow \alpha ||\frac{K-1}{2}e - sg(z)||^2$
-

The loss term  $L_{comm}$  is added to the loss function of the language model for optimization. Then the complete loss function formulates as:

$$L(Y, \hat{Y}) = CrossEntropy(Y, \hat{Y}) + \alpha L_{comm}$$

where  $Y$  is ground truth and  $\hat{Y}$  is model prediction.  $\alpha$  is a tuned parameter.

### 3.2 Optimal Bit width

To determine the optimal quantization bit width  $b$ , where discrete representation levels  $K = 2^b$ , we exploited feature's probability distribution, proposed a selection protocol based on Shannon's source coding theorem [22], which is formulate as:

**Theorem.** Let  $\Sigma_1, \Sigma_2$  denote two finite alphabets, and let  $\Sigma_1^*$  and  $\Sigma_2^*$  denote the sets of all finite words from those alphabets, respectively.

Suppose that  $X$  is a random variable taking values in  $\Sigma_1$ , and let  $f$  be a uniquely decodable code from  $\Sigma_1^*$  to  $\Sigma_2^*$ , where  $|\Sigma_2| = a$ . Let  $S$  denote the random variable representing the length of the codeword  $f(X)$ .

If  $f$  is optimal in the sense that it minimizes the expected word length for  $X$ , then

$$\frac{H(X)}{\log_2 a} \leq \mathbb{E}[S] < \frac{H(X)}{\log_2 a} + 1. \quad (1)$$

The theorem implies that for a  $d$ -dimensional embedding, when using binary storage, one can construct a discrete encoding by assigning  $H(X)$  bits to each dimension that is theoretically able to retain the entire embedding without information loss. We assume that the source data is identically distributed with a probability density function  $p(x)$ , then the theoretical optimal bit width is formulated as:

$$H(X) = \int -p(x) \log p(x) dx$$

$$b \geq H(x)$$

Since the true probability distribution function  $p(x)$  is not obtainable, we used the Gaussian kernel density estimation method to approximate it. Next, we justified that the kernel density estimator provides a practical means to estimate the information entropy, thereby enabling the determination of an appropriate quantization bit resolution. Here, we choose Scott's Rule, a common bandwidth selection method minimizing its mean integrated squared error (MISE) [23]:

$$h = \left(\frac{4}{3}\right)^{1/5} \cdot \sigma \cdot n^{-1/5}$$

$$\hat{p}(x) = \frac{1}{nh} \sum_{i=1}^n \varphi\left(\frac{x - X_i}{h}\right)$$

$$\hat{H}(x) = \int -\hat{p}(x) \log \hat{p}(x) dx$$

where  $\varphi(u) = \frac{1}{\sqrt{2\pi}} e^{-u^2/2}$ ,  $n$  is sample size and  $\sigma$  is sample standard error.

The estimator is asymptotically unbiased as demonstrated by Gao et al. [24], which is shown detailedly in appendix B. This indicates that, given a sufficiently large sample of source features, it provides a consistent and reliable estimate of entropy, thereby enabling a principled determination of the bit width.

### 3.3 Model Architecture

Based on the framework of TinyLLaVA, we presented a new foundation model structure that involves quantization techniques. As illustrated in Figure 1, our model is designed to encode both visual and textual inputs efficiently.

**Vision Tower** The vision tower  $\mathcal{V}$  takes an image  $X$  with dimension  $[B, C, H, W]$  as input, where  $B$  is batch size,  $C$  is number of channels,  $H, W$  are the height and width, and outputs a sequence of image patch features

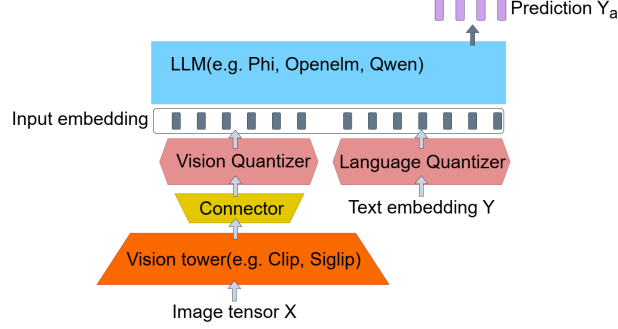


Figure 1: Overview of model architecture: (a). Vision tower for image encoding. (b). Connector for modality alignment. (c). Vision quantizer and language quantizer for feature compression and reconstruction. (d). Large language model for downstream tasks.

$\mathcal{V}(X) = \{v_i \in R^d\}_{i=1}^N$  with shape  $[B, N, d]$ . It can be either vision transformer model (ViT) or a deep convolutional neural network (CNN) for feature extraction.

**Connector** The connector  $\mathcal{P}_\theta$  maps vision modal features to language modal features. Its input is an image patch feature sequence produced by Vision Tower  $\{v_i \in R^D\}_{i=1}^N$  which is mapped into the corresponding language feature space  $\{h_i \in R^D\}_{i=1}^N$ . The common used connector is an MLP.

### Quantizer

The architecture of the quantizer  $Q_\varphi$  is illustrated in Figure 2. Since the multimodal foundation model already incorporates an encoder-decoder structure, we introduce only a single linear transformation to facilitate discrete representation learning. The quantizer first maps input features into a low-bit integer space via quantization, enabling efficient transmission, and then reconstructs them back into the feature space for further processing. Notably, this quantizer is deployed on both the client and the central server: the client generates the integer representations, which are then reconstructed on the server. To accommodate the unique characteristics of each modality, we assign a separate quantizer to each modality.

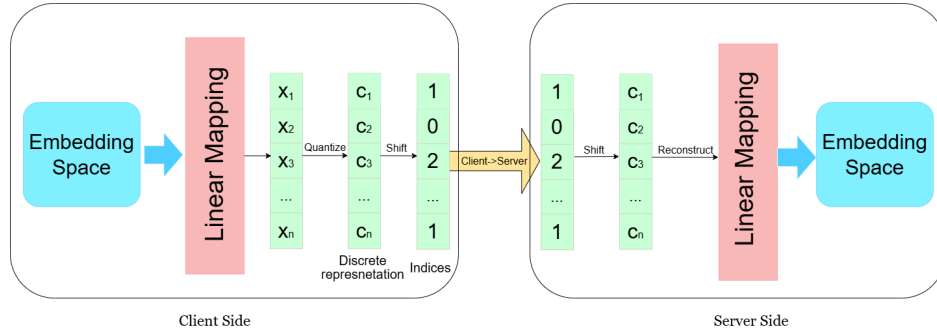


Figure 2: The quantizer  $Q_\varphi$  consists of a client part and a server part. The client maps intermediate features into low-bit integer indices, while the server reconstruct these indices back into features for the subsequent model.

**Language model** Language model  $\mathcal{L}_\omega$  takes an embedding sequence  $\{h_i \in R^D\}_{i=1}^M$  as input, and outputs the corresponding prediction. A quantizer and embedding module are usually associated with the language model to map the input of a word sequence into the embedding space and also from embedding space to word sequence.

### 3.4 Training strategy

We inherited the training strategy from TinyLLaVA [7] and adopted the two-stage training strategy of TinyLLaVA, feature-alignment pretraining and supervised fine-tuning. Each stage is trained to convergence in a single epoch on the corresponding dataset.

**pretraining** The model is pretrained in order to align text and image features. The data consist of pairs  $(X, Y_a)$ , where  $X$  is the image and  $Y_a$  is the description of the image. The model is trained to generate the correct description given an image.

**fine-tuning** The model is given  $(X, Y)$ , where  $X$  is an image and  $Y = \{Y_q^t, Y_a^t\}_{t=1}^T$  is a set of conversation where  $Y_q^t$ 's are user's questions and  $Y_a^t$ 's are answers. The model is trained to predict answer autoregressively given all previous conversations.

## 4 Experiment

### 4.1 Experiment settings

#### 4.1.1 Model architecture

In our experiment, we selected SigLip-SO400M [16] as the vision tower, OpenELM-270M [14] as the language model, both loaded with their pretrained weights, and a two-layer MLP with GELU activation functions as the connector. To investigate the quantization effect, we benchmarked FSQ quantizer, our modified quantizer and empty quantizer (no quantization) for comparison.

#### 4.1.2 Training data

We used the dataset proposed in LLaVA-1.5 [25] for training. The dataset consists of 558K images with captions, and 665K images with visual-instructed conversations for fine tuning.

#### 4.1.3 Training recipes

We adopted the base recipe presented by TinyLLaVA [7]. During pretraining, only the connector and quantizer's parameters are tuned and we set the learning rate at  $5e^{-4}$  and batch size at 32. During fine-tuning, the language model, connector and quantizer are tuned, and we set learning rate at  $2e^{-5}$  and batch size at 8.

#### 4.1.4 Baseline Methods

We compared our discrete learning framework with multiple data compression methods as follows:

##### Original model

To illustrate the efficiency of our method, we first evaluated the performance of the original model without any reduction in features. Our experiments showed that the proposed method achieves performance comparable to the original model while substantially reducing transmission cost.

##### FSQ

FSQ [6] is discrete learning methods using encoder-decoder structure and rounding operations, as demonstrated in previous sections.

##### Top-k Sparsification

Top-k sparsification [10] reduces data transmission by selecting the  $k$  elements with the highest probabilities, while retaining a small chance of sampling non-top- $k$  elements to preserve feature diversity.

##### Compression rate settings

We compared above baseline methods under multiple data compression rate. In our experiments, we uses FP16 to accelerate training. Therefore, each dimension of every embedding is represented in FP16 format and occupies 16 bits. Let  $d$  be the number of discrete representation levels in FSQ and our method,  $K$  be the selected features in Top-K sparsification,  $H$  be the number of embedding dimensions. Then the data compression rates are defined as in table.1:

Table 1: Compression rate definition of different methods

Method	Compression rate
Discrete learning	$\frac{16}{d}$
Top-K Sparsification	$\frac{H}{K}$

#### 4.1.5 Evaluation benchmark

We tested the model’s performance with multiple benchmark datasets including VQAV2 [26], TextVQA [27], Pope [28], MMvet [29], and MME [30]. They cover a wide range of model functions including visual recognition, OCR and numerical reasoning. We further investigated the model’s ability in terms of both perceptual processing and cognitive reasoning.

### 4.2 Experiment result

#### 4.2.1 Optimal Quantization bandwidth

The optimal number of discrete representation levels was determined by investigating the probability distribution of the source features and computing the corresponding information entropy. For each feature, its distribution was estimated via Gaussian kernel density estimation based on the activation values from a batch; the entropy was then computed from this estimated distribution. To evaluate the robustness of the estimation, this process was repeated across numerous batches. The outcomes of this analysis are illustrated in table 2. Detailed experimental results are shown appendix A.

Table 2: Entropy estimation across 8 batches

Batch number	Estimated entropy
batch 1	1.8077
batch 2	1.838
batch 3	1.8023
batch 4	1.8281
batch 5	1.7989
batch 6	1.8402
batch 7	1.8327
batch 8	1.8328

These results indicate that a 2-bit discrete representation is theoretically sufficient for optimal performance. This finding remains consistent across different batches, confirming the robustness and reliability of the determination. We further validated this conclusion by examining the relationship between the benchmark performance and the quantization bandwidth, as shown in Figure 3.

The comparison reveals that our model, equipped with the proposed vector quantization method, achieves its optimal performance at 2 or 3 bits, consistent with the theoretical results obtained earlier. In contrast, the model using FSQ exhibits a significant performance gap under low-bit-rate conditions.

#### 4.2.2 Inference Examples

Some model inference results are shown in Figure 4.

#### 4.2.3 Comparison of perception

We evaluated the perceptual capability of each model, and the results in Table 3 show that learning-based methods consistently outperform top-K sparsification in terms of perception. Furthermore, our approach notably surpasses FSQ and closely approximates the performance of the original model even under low-bit representations.

Table 3: Model Perception Comparison

Model	VQAV2	TextVQA	Pope	MME (perception)	MMVet-rec	MMVet-ocr	MMVet-spat
Original model	73.04	44.98	85.7	1051	20.6	14.4	13.7
<b>Our Method</b> ( $8 \times$ compression)	72.11	42.98	85.6	1028	19.1	16.4	17.1
FSQ ( $8 \times$ compression)	67.92	38.52	83.0	935	20.3	11.2	11.3
Top-K Sparsification ( $8 \times$ compression)	64.55	36.12	80.7	923	17.8	12	13.9
<b>Our Method</b> ( $4 \times$ compression)	72.18	42.43	85.7	1067	21.3	16.2	18.4
FSQ ( $4 \times$ compression)	72.59	43.44	86.2	1050	19.7	13.7	15.6
Top-K Sparsification ( $4 \times$ compression)	71.99	40.82	84.5	1065	20.3	13.1	10.4



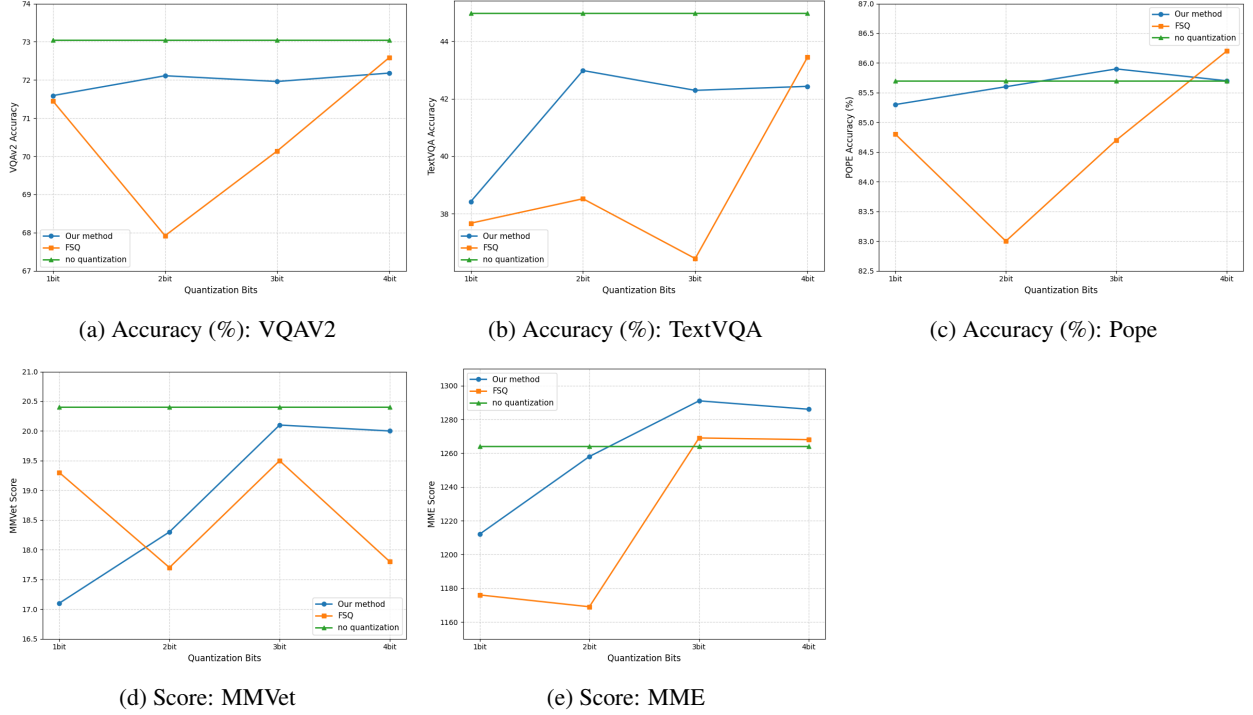


Figure 3: Model’s performance in 5 benchmarks across 1-5 bits. Our method achieves optimal performance at 2 or 3 bits.

#### 4.2.4 Comparison of cognition

We investigated model’s cognitive ability using the MME dataset. The results in Table 4 revealed a distinct pattern: compared with the original model, the quantized variant exhibited no significant performance degradation and, in fact, achieved superior cognition scores. This finding suggests that the model’s cognitive functions are less dependent on the complete preservation of information from the input data.

Table 4: Model Cognition Comparison

Model	MME(cognition)	MMVet-know	MMVet-gen	MMVet-math
Original model	213	6.8	7.9	3.8
<b>Our Method</b> ( $8 \times$ compression)	230	5.2	6.7	11.2
FSQ ( $8 \times$ compression)	234	10	7	3.8
Top-K Sparsification ( $8 \times$ compression)	232	7.1	4.6	8.1
<b>Our Method</b> ( $4 \times$ compression)	219	8	6.7	3.8
FSQ ( $4 \times$ compression)	218	8.5	6.9	3.5
Top-K Sparsification ( $4 \times$ compression)	210	7.5	7	4.6

## 5 Conclusion

In our study, we presented a novel multi-modal foundation model structure that integrates the quantization technique to enable efficient split learning. In our experiment, we demonstrated that our model preserves most performance while requiring only the transmission of low-bit integer features across the network. We also presented a general framework for constructing, evaluating, and analyzing small scale multi-modal foundation model with quantization integrated.



(a) Question: What sport is being played? Answer the question using a single word or phrase. Answer: tennis



(b) Question: "Can you give a short introduction to this person?", Answer: "The image features a man with long, thick hair, wearing a black suit and a white shirt. He appears to be a prominent figure in the history of science, as he is described as a great scientist. The man's hair is described as long and thick, and he has a prominent forehead. The man's face is also prominent, with a prominent brow."



(c) Question: "Is the man going to fall down?" Answer: "No, the man is not going to fall down while running. He is running on a red road, which is a designated road for vehicles and pedestrians."

Figure 4: Model Inference examples

## References

- [1] Rishi Bommasani, Drew A. Hudson, Ehsan Adeli, Russ Altman, Simran Arora, Sydney von Arx, Michael S. Bernstein, Jeannette Bohg, Antoine Bosselut, Emma Brunskill, Erik Brynjolfsson, Shyamal Buch, Dallas Card, Rodrigo Castellon, Niladri Chatterji, Annie Chen, Kathleen Creel, Jared Quincy Davis, Dora Demszky, Chris Donahue, Moussa Doumbouya, Esin Durmus, Stefano Ermon, John Etchemendy, Kawin Ethayarajh, Li Fei-Fei, Chelsea Finn, Trevor Gale, Lauren Gillespie, Karan Goel, Noah Goodman, Shelby Grossman, Neel Guha, Tatsunori Hashimoto, Peter Henderson, John Hewitt, Daniel E. Ho, Jenny Hong, Kyle Hsu, Jing Huang, Thomas Icard, Saahil Jain, Dan Jurafsky, Pratyusha Kalluri, Siddharth Karamcheti, Geoff Keeling, Fereshte Khani, Omar Khattab, Pang Wei Koh, Mark Krass, Ranjay Krishna, Rohith Kuditipudi, Ananya Kumar, Faisal Ladhak, Mina Lee, Tony Lee, Jure Leskovec, Isabelle Levent, Xiang Lisa Li, Xuechen Li, Tengyu Ma, Ali Malik, Christopher D. Manning, Suvir Mirchandani, Eric Mitchell, Zanele Munyikwa, Suraj Nair, Avanika Narayan, Deepak Narayanan, Ben Newman, Allen Nie, Juan Carlos Nieves, Hamed Nilforoshan, Julian Nyarko, Giray Ogut, Laurel Orr, Isabel Papadimitriou, Joon Sung Park, Chris Piech, Eva Portelance, Christopher Potts, Aditi Raghunathan, Rob Reich, Hongyu Ren, Frieda Rong, Yusuf Roohani, Camilo Ruiz, Jack Ryan, Christopher Ré, Dorsa Sadigh, Shiori Sagawa, Keshav Santhanam, Andy Shih, Krishnan Srinivasan, Alex Tamkin, Rohan Taori, Armin W. Thomas, Florian Tramèr, Rose E. Wang, William Wang, Bohan Wu, Jiajun Wu, Yuhuai Wu, Sang Michael Xie, Michihiro Yasunaga, Jiaxuan You, Matei Zaharia, Michael Zhang, Tianyi Zhang, Xikun Zhang, Yuhui Zhang, Lucia Zheng, Kaitlyn Zhou, and Percy Liang. On the opportunities and risks of foundation models, 2022.

- [2] Otkrist Gupta and Ramesh Raskar. Distributed learning of deep neural network over multiple agents, 2018.
- [3] Tim Dettmers, Mike Lewis, Younes Belkada, and Luke Zettlemoyer. Llm.int8(): 8-bit matrix multiplication for transformers at scale, 2022.
- [4] Jiawei Yang, Zhongbo Li, Zeqin Feng, and Yongqiang Xie. A survey on neural network quantization. In *Proceedings of the 2025 6th International Conference on Computer Information and Big Data Applications*, CIBDA '25, page 384–394, New York, NY, USA, 2025. Association for Computing Machinery.
- [5] Aaron van den Oord, Oriol Vinyals, and Koray Kavukcuoglu. Neural discrete representation learning, 2018.
- [6] Fabian Mentzer, David Minnen, Eirikur Agustsson, and Michael Tschannen. Finite scalar quantization: Vq-vae made simple, 2023.
- [7] Baichuan Zhou, Ying Hu, Xi Weng, Junlong Jia, Jie Luo, Xien Liu, Ji Wu, and Lei Huang. Tinyllava: A framework of small-scale large multimodal models, 2024.
- [8] Ngoc Duy Pham, Khoa T. Phan, and Naveen Chilamkurti. Enhancing accuracy-privacy trade-off in differentially private split learning. *IEEE Transactions on Emerging Topics in Computational Intelligence*, 9(1):988–1000, 2025.
- [9] Yukun Jiang, Peiran Wang, Chengguo Lin, Ziyue Huang, and Yong Cheng. Training on fake labels: Mitigating label leakage in split learning via secure dimension transformation, 2024.
- [10] Fei Zheng, Chaochao Chen, Lingjuan Lyu, and Binhui Yao. Reducing communication for split learning by randomized top-k sparsification. In *Proceedings of the Thirty-Second International Joint Conference on Artificial Intelligence*, IJCAI-2023, page 4665–4673. International Joint Conferences on Artificial Intelligence Organization, August 2023.
- [11] Yongjeong Oh, Jaeho Lee, Christopher G. Brinton, and Yo-Seb Jeon. Communication-efficient split learning via adaptive feature-wise compression, 2025.
- [12] Tom B. Brown, Benjamin Mann, Nick Ryder, Melanie Subbiah, Jared Kaplan, Prafulla Dhariwal, Arvind Nee-lakantan, Pranav Shyam, Girish Sastry, Amanda Askell, Sandhini Agarwal, Ariel Herbert-Voss, Gretchen Krueger, Tom Henighan, Rewon Child, Aditya Ramesh, Daniel M. Ziegler, Jeffrey Wu, Clemens Winter, Christopher Hesse, Mark Chen, Eric Sigler, Mateusz Litwin, Scott Gray, Benjamin Chess, Jack Clark, Christopher Berner, Sam McCandlish, Alec Radford, Ilya Sutskever, and Dario Amodei. Language models are few-shot learners, 2020.
- [13] Marah Abidin, Jyoti Aneja, Hany Awadalla, Ahmed Awadallah, Ammar Ahmad Awan, Nguyen Bach, Amit Bahree, Arash Bakhtiari, Jianmin Bao, Harkirat Behl, Alon Benhaim, Misha Bilenko, Johan Bjorck, Sébastien Bubeck, Martin Cai, Qin Cai, Vishrav Chaudhary, Dong Chen, Dongdong Chen, Weizhu Chen, Yen-Chun Chen, Yi-Ling Chen, Hao Cheng, Parul Chopra, Xiyang Dai, Matthew Dixon, Ronen Eldan, Victor Fragoso, Jianfeng Gao, Mei Gao, Min Gao, Amit Garg, Allie Del Giorno, Abhishek Goswami, Suriya Gunasekar, Emman Haider, Junheng Hao, Russell J. Hewett, Wenxiang Hu, Jamie Huynh, Dan Iter, Sam Ade Jacobs, Mojan Javaheripi, Xin Jin, Nikos Karampatziakis, Piero Kauffmann, Mahoud Khademi, Dongwoo Kim, Young Jin Kim, Lev Kurilenko, James R. Lee, Yin Tat Lee, Yuanzhi Li, Yunsheng Li, Chen Liang, Lars Liden, Xihui Lin, Zeqi Lin, Ce Liu, Liyuan Liu, Mengchen Liu, Weishung Liu, Xiaodong Liu, Chong Luo, Piyush Madan, Ali Mahmoudzadeh, David Majercak, Matt Mazzola, Caio César Teodoro Mendes, Arindam Mitra, Hardik Modi, Anh Nguyen, Brandon Norick, Barun Patra, Daniel Perez-Becker, Thomas Portet, Reid Pryzant, Heyang Qin, Marko Radmilac, Liliang Ren, Gustavo de Rosa, Corby Rosset, Sambudha Roy, Olatunji Ruwase, Olli Saarikivi, Amin Saied, Adil Salim, Michael Santacrose, Shital Shah, Ning Shang, Hiteshi Sharma, Yelong Shen, Swadheen Shukla, Xia Song, Masahiro Tanaka, Andrea Tupini, Praneetha Vaddamanu, Chunyu Wang, Guanhua Wang, Lijuan Wang, Shuohang Wang, Xin Wang, Yu Wang, Rachel Ward, Wen Wen, Philipp Witte, Haiping Wu, Xiaoxia Wu, Michael Wyatt, Bin Xiao, Can Xu, Jiahang Xu, Weijian Xu, Jilong Xue, Sonali Yadav, Fan Yang, Jianwei Yang, Yifan Yang, Ziyi Yang, Donghan Yu, Lu Yuan, Chenruidong Zhang, Cyril Zhang, Jianwen Zhang, Li Lyna Zhang, Yi Zhang, Yue Zhang, Yunan Zhang, and Xiren Zhou. Phi-3 technical report: A highly capable language model locally on your phone, 2024.
- [14] Sachin Mehta, Mohammad Hossein Sekhavat, Qingqing Cao, Maxwell Horton, Yanzi Jin, Chenfan Sun, Iman Mirzadeh, Mahyar Najibi, Dmitry Belenko, Peter Zatloukal, and Mohammad Rastegari. Openelm: An efficient language model family with open training and inference framework, 2024.
- [15] Qwen, :, An Yang, Baosong Yang, Beichen Zhang, Binyuan Hui, Bo Zheng, Bowen Yu, Chengyuan Li, Dayiheng Liu, Fei Huang, Haoran Wei, Huan Lin, Jian Yang, Jianhong Tu, Jianwei Zhang, Jianxin Yang, Jiayi Yang, Jingren Zhou, Junyang Lin, Kai Dang, Keming Lu, Keqin Bao, Kexin Yang, Le Yu, Mei Li, Mingfeng Xue, Pei Zhang, Qin Zhu, Rui Men, Runji Lin, Tianhao Li, Tianyi Tang, Tingyu Xia, Xingzhang Ren, Xuancheng Ren, Yang Fan, Yang Su, Yichang Zhang, Yu Wan, Yuqiong Liu, Zeyu Cui, Zhenru Zhang, and Zihan Qiu. Qwen2.5 technical report, 2025.

- [16] Michael Tschannen, Alexey Gritsenko, Xiao Wang, Muhammad Ferjad Naeem, Ibrahim Alabdulmohsin, Nikhil Parthasarathy, Talfan Evans, Lucas Beyer, Ye Xia, Basil Mustafa, Olivier Hénaff, Jeremiah Harmsen, Andreas Steiner, and Xiaohua Zhai. Siglip 2: Multilingual vision-language encoders with improved semantic understanding, localization, and dense features, 2025.
- [17] Alec Radford, Jong Wook Kim, Chris Hallacy, Aditya Ramesh, Gabriel Goh, Sandhini Agarwal, Girish Sastry, Amanda Askell, Pamela Mishkin, Jack Clark, Gretchen Krueger, and Ilya Sutskever. Learning transferable visual models from natural language supervision, 2021.
- [18] Haotian Liu, Chunyuan Li, Qingyang Wu, and Yong Jae Lee. Visual instruction tuning, 2023.
- [19] Tim Dettmers, Artidoro Pagnoni, Ari Holtzman, and Luke Zettlemoyer. Qlora: Efficient finetuning of quantized llms, 2023.
- [20] Ali Razavi, Aaron van den Oord, and Oriol Vinyals. Generating diverse high-fidelity images with vq-vae-2, 2019.
- [21] Patrick Esser, Robin Rombach, and Björn Ommer. Taming transformers for high-resolution image synthesis, 2021.
- [22] C. E. Shannon. A mathematical theory of communication. *The Bell System Technical Journal*, 27(3):379–423, 1948.
- [23] David W Scott. *Multivariate density estimation: theory, practice, and visualization*. John Wiley & Sons, 2015.
- [24] Shuyang Gao, Greg Ver Steeg, and Aram Galstyan. Estimating mutual information by local gaussian approximation. In *Proceedings of the Thirty-First Conference on Uncertainty in Artificial Intelligence, UAI’15*, page 278–287, Arlington, Virginia, USA, 2015. AUAI Press.
- [25] Haotian Liu, Chunyuan Li, Yuheng Li, and Yong Jae Lee. Improved baselines with visual instruction tuning, 2024.
- [26] Ziheng Jia, Zicheng Zhang, Jiaying Qian, Haoning Wu, Wei Sun, Chunyi Li, Xiaohong Liu, Weisi Lin, Guangtao Zhai, and Xiongkuo Min. Vqa<sup>2</sup>: Visual question answering for video quality assessment, 2024.
- [27] Amanpreet Singh, Vivek Natarajan, Meet Shah, Yu Jiang, Xinlei Chen, Dhruv Batra, Devi Parikh, and Marcus Rohrbach. Towards vqa models that can read, 2019.
- [28] Yifan Li, Yifan Du, Kun Zhou, Jinpeng Wang, Wayne Xin Zhao, and Ji-Rong Wen. Evaluating object hallucination in large vision-language models, 2023.
- [29] Weihao Yu, Zhengyuan Yang, Linjie Li, Jianfeng Wang, Kevin Lin, Zicheng Liu, Xinchao Wang, and Lijuan Wang. Mm-vet: Evaluating large multimodal models for integrated capabilities, 2024.
- [30] Chaoyou Fu, Peixian Chen, Yunhang Shen, Yulei Qin, Mengdan Zhang, Xu Lin, Jinrui Yang, Xiawu Zheng, Ke Li, Xing Sun, Yunsheng Wu, and Rongrong Ji. Mme: A comprehensive evaluation benchmark for multimodal large language models, 2024.
- [31] N. L. Hjort and M. C. Jones. Locally parametric nonparametric density estimation. *The Annals of Statistics*, 24(4):1619 – 1647, 1996.

## Appendix A

This section showed detailed density and entropy estimation result.

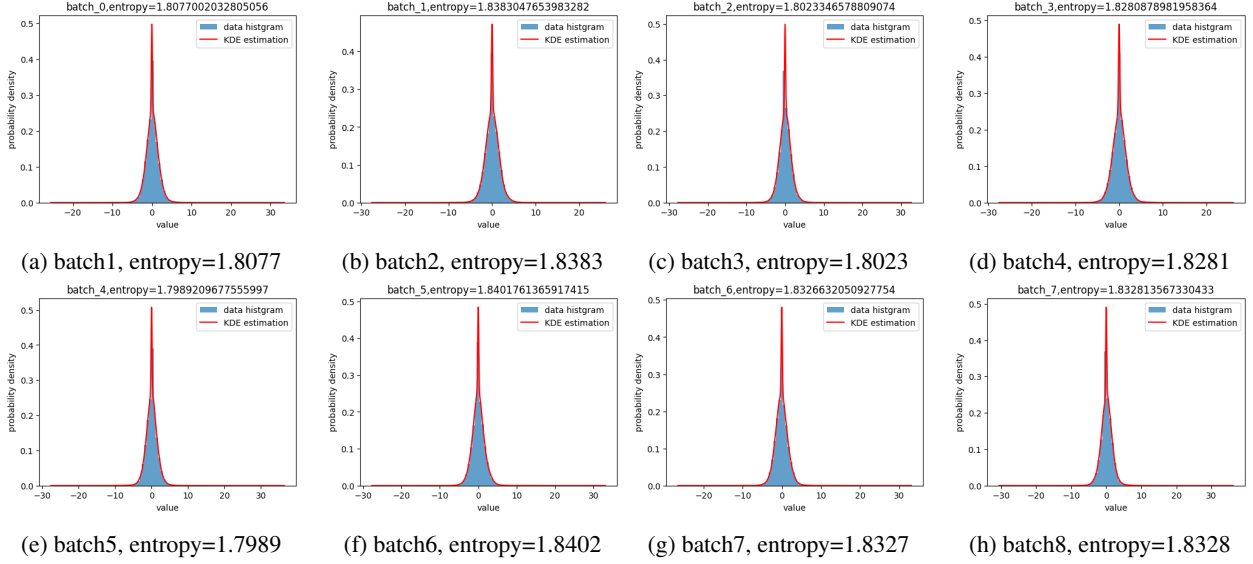


Figure A1: Estimation of Distribution and Entropy across 8 batches

## Appendix B

This section gives proof of the asymptotic unbiasedness of our entropy estimator. This proof was first proposed by Gao et al. [24].

Consider  $N$  i.i.d. samples  $(\mathcal{X})$  drawn from an unknown distribution  $f_X$ , where  $\mathbf{x}$  is random vector of dimensionality  $d$ , respectively. Let us construct the following estimators for entropy,

$$\hat{H}(\mathbf{x}) = -\frac{1}{N} \sum_{i=1}^N \log \hat{f}(\mathbf{x}_i), \quad (2)$$

Here  $\hat{f}(\mathbf{x})$  is the local Gaussian density estimators for  $f_X(\mathbf{x})$ . Which is defined as:

**Theorem B1** (Hjort and Jones, 1996 [31]). *Let  $\hat{f}(x)$  be the Local Gaussian Density Estimator with bandwidths  $h_i$  satisfying*

$$h_i \rightarrow 0, \quad Nh_i \rightarrow \infty.$$

*Then*

$$\lim_{N \rightarrow \infty} \mathbb{E}|\hat{f}(x) - f(x)| = 0, \quad \lim_{N \rightarrow \infty} \mathbb{E}|\hat{f}(x) - f(x)|^2 = 0.$$

**Theorem B2** (Lebesgue Dominated Convergence Theorem). *Let  $\{f_N\}$  be a sequence of functions such that  $f_N(x) \rightarrow f(x)$  pointwise for any  $x \in \mathbb{R}^d$ . Assume further that  $f_N$  is dominated by an integrable function  $g$ , i.e.,*

$$|f_N(x)| \leq g(x), \quad \forall x.$$

*Then,*

$$\lim_{N \rightarrow \infty} \int |f_N(x) - f(x)| dx = 0.$$

**Theorem B3** (Asymptotic Unbiasedness of Entropy Estimator). *If the conditions in Eq. 9 hold, then the entropy estimator given by Eq. 12 is asymptotically unbiased, i.e.,*

$$\lim_{N \rightarrow \infty} \mathbb{E} \hat{H}(x) = H(x).$$

*Proof.* Consider  $N$  i.i.d. samples  $\{x^{(i)}\}_{i=1}^N$  drawn from the density  $f(x)$ , and let  $F_N(x)$  denote the empirical distribution. Define

$$H_1 = -\frac{1}{N} \sum_{i=1}^N \ln \mathbb{E} \hat{f}(x_i), \quad (3)$$

$$H_2 = -\frac{1}{N} \sum_{i=1}^N \ln f(x_i). \quad (4)$$

Then

$$\mathbb{E}|\hat{H}(x) - H(x)| \leq \mathbb{E}|\hat{H} - H_1| + \mathbb{E}|H_1 - H_2| + \mathbb{E}|H_2 - H|. \quad (*)$$

We show that each term in  $(*)$  converges to 0 as  $N \rightarrow \infty$ .

**(1) Convergence of  $\mathbb{E}|\hat{H} - H_1|$**  By the mean value theorem, for each  $x$  there exists  $t_x \in (0, 1)$  such that

$$\ln \hat{f}(x) = \ln \mathbb{E} \hat{f}(x) + (\hat{f}(x) - \mathbb{E} \hat{f}(x)) \ln'(t_x \hat{f}(x) + (1 - t_x) \mathbb{E} \hat{f}(x)).$$

Then

$$\begin{aligned} \mathbb{E}|\hat{H} - H_1| &= \mathbb{E} \left| \int [\ln \hat{f}(x) - \ln \mathbb{E} \hat{f}(x)] dF_N(x) \right| \\ &\leq \frac{1}{1-t} \mathbb{E} \left( \frac{1}{N} \sum_{i=1}^N \frac{|\hat{f}(x_i) - \mathbb{E} \hat{f}(x_i)|}{\mathbb{E} \hat{f}(x_i)} \right) \\ &= \frac{1}{1-t} \int \frac{|\hat{f}(u) - \mathbb{E} \hat{f}(u)|}{\mathbb{E} \hat{f}(u)} f(u) du. \end{aligned}$$

Using Theorem B1,  $\hat{f}(u) \rightarrow f(u)$  in  $L_1$ , hence the integrand goes to 0 and is dominated by  $2f(u)$ . Applying Theorem B2 yields

$$\lim_{N \rightarrow \infty} \mathbb{E}|\hat{H} - H_1| = 0.$$

**(2) Convergence of  $\mathbb{E}|H_1 - H_2|$**  Similarly, by the mean value theorem there exists  $t'_x \in (0, 1)$  such that

$$\ln \mathbb{E} \hat{f}(x) = \ln f(x) + (\mathbb{E} \hat{f}(x) - f(x)) \ln'(t'_x f(x) + (1 - t'_x) \mathbb{E} \hat{f}(x)).$$

Arguing as above,

$$\mathbb{E}|H_1 - H_2| \leq \frac{1}{t'} \int |\mathbb{E} \hat{f}(x) - f(x)| dx.$$

Again, by Theorem B1 and Theorem B2 the integrand converges to 0 and is dominated by  $2f(x)$ . Hence,

$$\lim_{N \rightarrow \infty} \mathbb{E}|H_1 - H_2| = 0.$$

**(3) Convergence of  $\mathbb{E}|H_2 - H|$**  We have

$$\mathbb{E}H_2 = -\mathbb{E}[\ln f(x)] = H(x),$$

so

$$\lim_{N \rightarrow \infty} \mathbb{E}|H_2 - H| = 0.$$

Combining the three parts proves that

$$\lim_{N \rightarrow \infty} \mathbb{E}|\hat{H}(x) - H(x)| = 0,$$

i.e., the entropy estimator is asymptotically unbiased.  $\square$